

Single-folding model for the spin-orbit potential between ^{19}F and ^{28}Si

M. B. Golin* and S. Kubono†

Brookhaven National Laboratory, Upton, New York 11973

(Received 7 May 1979)

A general expression for the spin-orbit potential between two heavy ions is derived using the single-folding method. This expression is applied to the calculation of the spin-orbit potential between ^{19}F and ^{28}Si , using single-particle as well as cluster model wave functions for ^{19}F . In the cluster model, the magnitude of the $^{19}\text{F} + ^{28}\text{Si}$ spin-orbit potential at the strong absorption radius is enhanced by a factor of 50 over the single-particle model estimate.

[NUCLEAR REACTIONS $^{19}\text{F} + ^{28}\text{Si}$ spin-orbit potential: single-folding method,
single-particle, and cluster model wave functions for ^{19}F .]

There is currently a lot of interest¹⁻⁶ in the magnitude of the spin-orbit potential for heavy ions. The transfer reaction data¹ and the polarization data² can only be reproduced by adding a significant spin-orbit term to the optical potential. However, in some cases such as $^{19}\text{F} + ^{28}\text{Si}$, the empirical result¹ is two orders of magnitude larger than the value obtained theoretically.^{4,5} So far, all the calculations^{4,5} were performed assuming a single-particle harmonic oscillator wave function for ^{19}F .

In the present note, we derive a general expression for the spin-orbit potential between two heavy ions using the single-folding model. We apply this expression to ^{19}F , assuming three different types of wave functions: a single-particle harmonic oscillator eigenfunction, a single-particle Woods-Saxon eigenfunction, and a $t + ^{16}\text{O}$ cluster model wave function. The first two give approximately the same result for the $^{19}\text{F} + ^{28}\text{Si}$ spin-orbit potential at the strong absorption radius.⁷ Clustering enhances the value of the spin-orbit potential by a factor of 50.

Let us briefly review the model. Consider a target of mass A_t and spin zero, and a projectile of mass A_p and spin \vec{S} . Suppose that the projectile can be described in terms of a cluster of mass A_c and spin \vec{s} , moving in a relative Ns state $\psi_c(\vec{r})$ around a spin zero core. N is the number of nodes allowed by the shell model for the relative motion. When the spin-orbit potential $v_{is}(x)$ between the cluster and the target is known, the spin-orbit potential $V_{LS}(R)$ between the projectile and the target can be evaluated in the single-folding model. Extending the method of Ref. 3 to take into account any cluster of mass A_c , we have

$$\vec{L} \cdot \vec{S} V_{LS}(R) = \vec{I} \cdot \vec{s} \int d^3r |\psi_c(\vec{r})|^2 v_{is}(x), \quad (1)$$

where the coordinates \vec{R} , \vec{r} , and \vec{x} are shown in

Fig. 1, \vec{L} is the orbital angular momentum of the projectile with respect to the target, and \vec{I} is the orbital angular momentum of the cluster with respect to the target.

Neglecting the velocity of the cluster around the projectile core, we can approximate the orbital angular momentum of the cluster by

$$\vec{I} = \frac{A_c}{A_p} \vec{P} \times \vec{R} + \frac{A_c(A_p - A_c)}{A_p} \vec{P} \times \vec{r}, \quad (2)$$

where \vec{P} is the projectile momentum.

The first term in Eq. (2) is proportional to the projectile angular momentum L . We shall denote by $V_{LS,1}(R)$ the contribution of this term to the heavy-ion spin-orbit potential

$$V_{LS,1}(R) = \frac{A_c}{A_p} \int d^3r |\psi_c(\vec{r})|^2 v_{is}(x). \quad (3)$$

The contribution of the second term can be easily evaluated using the heavy-ion approximation

$$\vec{r} \cong \frac{(\vec{R} \cdot \vec{r})}{R^2} \vec{R},$$

which leads to

$$V_{LS,2}(R) \cong \frac{A_c(A_p - A_c)}{A_p^2 R} \int d^3r |\psi_c(\vec{r})|^2 r \cos\theta v_{is}(x). \quad (4)$$

The spin-orbit potential $V_{LS}(R)$ between the projectile and the target is given by the sum

$$V_{LS}(R) = V_{LS,1}(R) + V_{LS,2}(R). \quad (5)$$

For the cluster-target spin-orbit potential $v_{is}(x)$, we use the standard parametrization

$$v_{is}(x) = 2 \left(\frac{\hbar}{m_p c} \right)^2 \frac{V_0}{x} \frac{df}{dx}, \quad (6a)$$

where

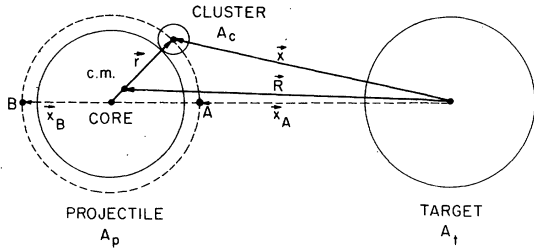


FIG. 1. Notation used for the coordinates \vec{R} , \vec{r} , \vec{x} , \vec{x}_A , and \vec{x}_B throughout this work.

$$f(x) = \frac{1}{1 + \exp[(x - R_{1s})/a_{1s}]} \quad (6b)$$

Inserting this expression for $v_{1s}(x)$ in Eqs. (3) and (4), and performing the integrations, we obtain

$$V_{LS,1}(R) = \left(\frac{\hbar}{m_p c}\right)^2 \frac{A_c}{(A_p - A_c)} [f(x_B) - f(x_A)] \times \frac{V_0}{R} \int_0^\infty r |\mathcal{R}_c(r)|^2 dr \quad (7)$$

and

$$V_{LS,2}(R) \cong -\frac{1}{4} \left(\frac{\hbar}{m_p c}\right)^2 \frac{A_c(A_p - A_c)}{A_p^2} \frac{1}{x_A} \frac{df}{dx_A} \times \frac{V_0}{R} \int_0^\infty r^3 |\mathcal{R}_c(r)|^2 dr, \quad (8)$$

where $\mathcal{R}_c(r)$ is the radial part of $\psi_c(\vec{r})$,

$$x_A = R - \frac{A_p - A_c}{A_p} r \quad (9a)$$

and

$$x_B = R + \frac{A_p - A_c}{A_p} r. \quad (9b)$$

Let us now apply this model to the ^{19}F projectile and ^{28}Si target.

We use initially a $p + ^{18}\text{O}$ single-particle wave function for ^{19}F , setting $A_c = 1$ in Eqs. (7) and (8). We adopt a $1s_{1/2}$ harmonic-oscillator eigenfunction for the proton, and determine the oscillator constant $\alpha = 0.645 \text{ fm}^{-1}$ by fitting the experimental rms radius⁸ of ^{19}F , $r = 2.9 \text{ fm}$. For the $v_{1s}(x)$ potential between the proton and the ^{28}Si target, we use the standard parametrization,⁹ $V_0 = 6.0 \text{ MeV}$, $R_{1s} = 3.067 \text{ fm}$, and $a_{1s} = 0.75 \text{ fm}$. At the strong absorption radius,⁷ $R_s = 1.5(A_p^{1/3} + A_t^{1/3}) \text{ fm}$, the $^{19}\text{F} + ^{28}\text{Si}$ spin-orbit potential of Eq. (5) is

$$V_{LS}(R_s) = (-1.2 + 0.3) \text{ keV} = -0.9 \text{ keV}. \quad (10)$$

The behavior of $V_{LS}(R)$ in the vicinity of the strong absorption radius is shown in Fig. 2.

In order to investigate whether this result is strongly dependent on the type of wave function

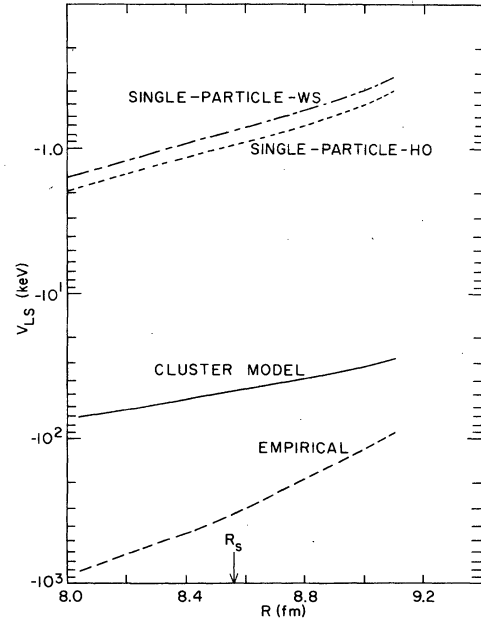


FIG. 2. The spin-orbit potential for $^{19}\text{F} + ^{28}\text{Si}$ in the vicinity of the strong absorption radius. The dash-dotted line and the dotted line are obtained using a single-particle wave function for ^{19}F . The dash-dotted line corresponds to a Woods-Saxon eigenfunction, and the dotted line to a harmonic-oscillator eigenfunction. The solid line is obtained assuming a cluster-model wave function for ^{19}F , and the dashed line is the empirical¹ spin-orbit potential for $^{19}\text{F} + ^{28}\text{Si}$.

used for the proton, we perform the same calculation using a $1s_{1/2}$ Woods-Saxon eigenfunction. We set the radius of the Woods-Saxon well at 2.9 fm and the diffusivity at 0.64 fm. We adjust the depth of the Woods-Saxon well to reproduce the 8 MeV separation energy of the proton in ^{19}F , taking into account the Coulomb potential of a spherical charge distribution of radius 2.9 fm. With this new single-particle wave function for ^{19}F , the $^{19}\text{F} + ^{28}\text{Si}$ spin-orbit potential at the strong absorption radius is

$$V_{LS}(R_s) = (-1.0 + 0.3) \text{ keV} = -0.7 \text{ keV}. \quad (11)$$

Therefore, the type of wave function used for the proton does not seem to have a large effect on the heavy-ion spin-orbit potential (see Fig. 2).

From earlier work,¹⁰⁻¹² it is well known that clustering effects are significant in ^{19}F . For instance, the cluster model¹² accounts successfully for the excitation energies, charge radii, quadrupole moments, and $E2$ and $M1$ transition rates in ^{19}F that cannot be explained in terms of a single-particle wave function. Therefore, it is also important to investigate the effect of clustering on the $^{19}\text{F} + ^{28}\text{Si}$ spin-orbit potential.

In the single-folding model developed above, we can easily introduce the $t + {}^{16}\text{O}$ wave function.¹² The triton spin-orbit potential $v_{is}(x)$ is known from the recent asymmetry measurements on a variety of targets.^{13,14} The parametrization which leads to the smallest χ^2 per point in the analyzing power and the cross section data is of the form^{13,14} $V_0 = 6$ MeV, $R_{ts} = 5.15$ fm, and $a_{ts} = 0.8$ fm. (If the depth V_0 were lowered¹⁵ to 2 MeV, or raised to 12 MeV, and the geometry kept fixed, the value of χ^2 per point would increase by a factor of 4,¹⁴ nearly independent of the target.) In order to calculate the wave function $\psi_c(\vec{r})$, we make the standard assumption that the triton cluster is moving around the ${}^{16}\text{O}$ core in a $3s_{1/2}$ orbit with binding energy 11.73 MeV, and we adopt the cluster-core potential of Ref. 12. The value of A_c in Eqs. (7) and (8) is now $A_c = 3$, and the cluster-core rms radius¹² is $r = 4.0$ fm. The resulting ${}^{19}\text{F} + {}^{28}\text{Si}$ spin-orbit potential at the strong absorption radius is

$$V_{LS}(R_s) = (-57 + 10) \text{ keV} = -47 \text{ keV}, \quad (12)$$

which is 50 times stronger than the value obtained

in Eqs. (10) and (11) using the single-particle model (see Fig. 2).

This large enhancement in $V_{LS}(R_s)$ is due, in part, to a larger cluster mass. It is also due to the geometry of the triton-target spin-orbit potential combined with the cluster-core distance in the ${}^{19}\text{F}$ wave function.

In conclusion, our phenomenological approach indicates that the $t + {}^{16}\text{O}$ model wave function for ${}^{19}\text{F}$ enhances the ${}^{19}\text{F} + {}^{28}\text{Si}$ spin-orbit potential by a factor of 50 over the single-particle estimate near the strong absorption radius. However, the cluster model result is still about a factor of 7 smaller than the empirical¹ spin-orbit strength.

We are grateful to Professor P. J. Ellis and Professor W. J. Thompson for several useful references, and to Dr. R. A. Hardekopf for making his results available before publication. This work was supported by the Division of Basic Science, Department of Energy, under Contract No. EY-76-C-02-0016.

*P. O. Box 406, BNL, Upton, New York 11973.

†Present address: Institute for Nuclear Study, Univ. of Tokyo, Tanashi, Tokyo, 188 Japan.

¹S. Kubono *et al.*, Phys. Rev. Lett. **38**, 817 (1977).

²W. Weiss *et al.*, Phys. Lett. **61B**, 237 (1976).

³H. Amakawa and K.-I. Kubo, Nucl. Phys. **A266**, 521 (1976).

⁴W. J. Thompson, in *Proceedings of the Rochester Symposium on Heavy-Ion Elastic Scattering, Rochester, 1977*, edited by R. M. DeVries, p. 321; in *Proceedings of the International Conference on Reactions between Complex Nuclei, Nashville, Tennessee, 1974*, edited by R. L. Robinson, F. K. McGowan, J. B. Ball, and J. H. Hamilton (North-Holland, Amsterdam, 1974), Vol. 1, p. 14.

⁵F. Petrovich, D. Stanley, L. A. Parks, and P. Nagel, Phys. Rev. C **17**, 1642 (1978).

⁶P. J. Moffa, Phys. Rev. C **16**, 1431 (1977).

⁷G. R. Satchler, in *Proceedings of the International Conference on Reactions between Complex Nuclei, Nashville, Tennessee, 1974*, edited by R. L. Robinson, F. K. McGowan, J. B. Ball, and J. H. Hamilton (North-Holland, Amsterdam, 1974), Vol. 2, p. 171.

⁸C. W. de Jaeger, H. de Vries, and C. de Vries, At. Data Nucl. Data Tables **A14**, 479 (1977).

⁹F. D. Becchetti, Jr. and G. W. Greenlees, Phys. Rev. **182**, 1190 (1969).

¹⁰P. J. Ellis and T. Engeland, Nucl. Phys. **A144**, 161 (1970).

¹¹N. Anyas-Weiss *et al.*, Phys. Rep. **12C**, 201 (1974).

¹²B. Buck and A. Pilt, Nucl. Phys. **A280**, 133 (1977).

¹³R. A. Hardekopf, L. R. Veaser, and P. W. Keaton, Jr., Phys. Rev. Lett. **35**, 1623 (1975).

¹⁴R. A. Hardekopf, private communication.

¹⁵S. Mordechai and H. T. Fortune, J. Phys. G: Nucl. Phys. **7**, 1177 (1978).